

Star-Forming Nuclear Rings in Spiral Galaxies

Jesús Falcón-Barroso¹
 Torsten Böker¹
 Eva Schinnerer²
 Johan H. Knapen³
 Stuart Ryder⁴

¹ European Space Agency, Noordwijk, the Netherlands,

² Max-Planck-Institut für Astronomie, Heidelberg, Germany

³ Instituto de Astrofísica de Canarias, Tenerife, Spain

⁴ Anglo-Australian Observatory, Epping, Australia

The study of gas transport to the inner regions of galaxies is a fundamental aspect in our understanding of the way galaxies evolve. In this context, star-forming nuclear rings are key features as they contain large amounts of gas and are the sites where a significant fraction of the current star formation is taking place in their host galaxies. Here we present some results from a study of how star formation progresses along nuclear star-forming rings in five spiral galaxies, based on near-infrared SINFONI integral-field observations at the VLT.

Nuclear Rings

The basic picture of how nuclear rings form is well established, both from a theoretical and an observational perspective (see Buta and Combes 1996 for a review). They are usually associated with the interplay between bar-driven gas inflow and the bar resonances. Perturbations in the gravitational potential, nearly always due to the presence of a stellar bar or oval distortion, causes the gas to lose angular momentum and spiral in towards the nucleus. Because of its dissipative nature, gas accumulates at the radii where the stellar orbits experience dynamical resonances with the rotating bar potential. In the case of the nuclear rings discussed here, this gas accumulation typically happens at the so-called Inner Lindblad resonance. When observed in more detail, the gas is found to enter the ring via two tightly wound spiral arms or dust lanes. At the contact points between the dust lanes and the ring, the gas be-

comes less turbulent, and enters almost circular orbits, which delineate the ring. While it is clear that there is abundant (molecular) gas throughout the ring, there has been an on-going debate about how and where star formation occurs.

Integral-field observations of nuclear rings

Integral-field spectroscopy allows the simultaneous measurement of a large number of spectra over a two-dimensional field of view. We used SINFONI *H*- and *K*-band spectroscopy to study the two-dimensional morphology and kinematics of star-forming nuclear rings in five spiral galaxies drawn from a large sample of galaxies observed in $H\alpha$ by Knapen et al. (2006). In Figure 1 we show a colour-composite image of one of the galaxies in our sample (NGC 613), highlighting the main structural features and in particular the nuclear ring discussed in the following.

Figure 2 shows the intensity and velocity maps for some of the most prominent spectral features in NGC 613. The $B\gamma$ emission shows a clearly defined ring structure, composed of seven almost regularly spaced bright clumps that are the sites of current massive star formation. These ‘hot spots’ are brightest along the southern half of the ring, while the northern half shows a well-defined ‘gap’ at PA 30° which is also evident in the $[\text{Fe II}]$ emission map. This direction agrees

well with that of the radio jet found by Hummel et al. (1987). It thus appears that a mechanical outflow from the central active black hole has disturbed the ring morphology.

H_2 emission is also apparent in the nuclear ring, but is strongest in the nucleus. The H_2 in the ring is not composed of distinct hot spots like the $B\gamma$ emission, but is more smoothly distributed. There are two emission peaks, found on opposite sides of the ring, at approximate PAs of 90° and 270° . If the H_2 emission in the ring of NGC 613 were caused purely by UV radiation, one might expect a spatial correspondence between H_2 and the ionised gas traced by $B\gamma$ and/or He I . However, many of the $B\gamma$ hot spots are not bright in H_2 . Therefore, the H_2 emission probably contains a non-negligible contribution from shock-heated molecular gas.

The nuclear spectrum shown in the bottom panel of Figure 2 highlights the presence of molecular emission (H_2) and the complete absence of hydrogen recombination lines (e.g. $B\gamma$). In contrast, the nuclear spectra of the remaining galaxies in our sample (not shown here) appear rather quiescent, i.e. their spectra are devoid of any line emission. This is not unexpected in a scenario in which gas accumulates at the nucleus over time until a critical density is reached. Star formation is then triggered, but can continue only until the gas supply is consumed or the energetic outflow from supernova explo-

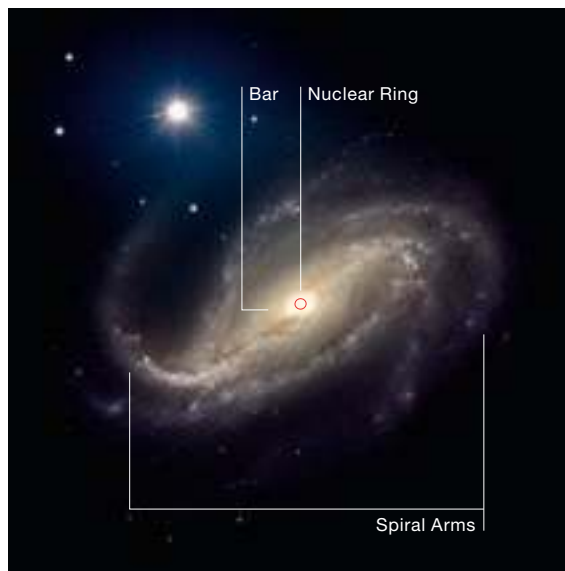


Figure 1: Colour-composite image of NGC 613 taken with FORS1 and FORS2 instruments (ESO Press Photo 33a/03). Labels highlight some of the main morphological features.

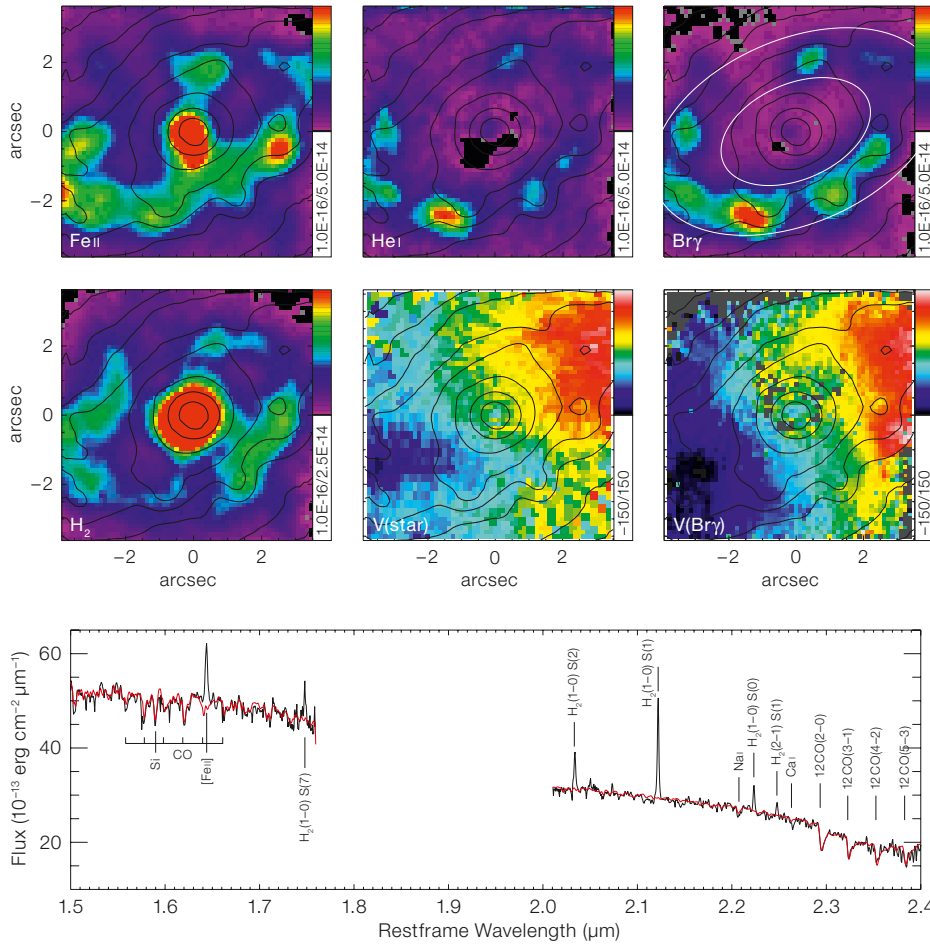


Figure 2: SINFONI near-infrared integral-field spectroscopy of NGC 613. Top row shows the morphology in the [FeII], HeI and Brackett- γ emission; lower row the H₂ emission morphology, the stellar kinematics (V(star)) and the Brackett- γ kinematics (V(Br γ)) of the nuclear ring in this galaxy. The black contours delineate the *K*-band light measured from the SINFONI observations while ellipses in the Br γ map delimit the extension of the ring. Bottom panel shows the nuclear spectrum of NGC 613 with the main spectral features highlighted.

value is well below typical detection limits ($\sim 1 \text{ \AA}$).

An alternative approach is to make use of several spectral lines, whose emission peaks at different cluster ages. In our case, we use the flux of three emission lines that are prominent in the NIR spectra of the star-forming regions in our sample of galaxies: HeI, Br γ , and [FeII]. Under the assumption that the underlying bulge/disc can be considered quiescent, and that most of the emission is produced in the ring itself, line fluxes are a better probe than the EWs. The reason is that EWs require an accurate knowledge of the continuum emission, not only for the hot spot itself, but also for the underlying bulge and/or disc, which is very hard to measure. The HeI and Br γ lines are both produced by photoionisation in the vicinity of hot O- or B-type stars. Given that the ionisation energy for the HeI line is higher than that of Br γ , it requires the presence of hotter and more massive stars, and hence its brightness falls off more rapidly after an instantaneous burst than that of the Br γ line. The time range covered by these two lines is from 0 to 10 Myr. Larger ages can be probed with the [FeII] line (a tracer of fast shocks produced in supernova remnants) whose contribution is almost constant from 3 to 35 Myr, and decreases sharply after that. Using the relative strength of those three lines, we are therefore able to probe ages in the range between 0 and 35 Myr, which represents a good match to the expected travel time of gas and star clusters along the nuclear ring.

Star formation along the rings

Figure 3 illustrates two plausible mechanisms that describe how star formation could proceed along the circumnuclear rings. In the first scenario, the *popcorn* model, gas enters the ring and accumu-

sions disrupts and/or expels the gas, thus ‘quenching’ the star formation. This scenario is entirely consistent with observations, at least for late-type spirals: only about 10 % of nuclear star clusters currently show emission lines, although most of them harbour a young stellar population of less than 100 Myr old (Rossa et al. 2006). This can naturally be explained if star formation in galactic nuclei is episodic in nature, with a duty cycle of about 10 %.

In Figure 2 we also show the stellar and ionised-gas kinematics for NGC 613. The stellar velocity field appears rather regular, despite the intense star formation within the nuclear ring. Because Br γ is generally the most prominent emission line in our data, we used it to make an estimate of the ionised gas kinematics. In all galaxies of our sample, the velocity gradients within the nuclear rings are smooth and the ionised gas has the same sense of rotation as the stars.

The ages of the stellar clusters

Measuring the relative ages of the different stellar clusters (i.e. hot spots) along the ring is a difficult task. The orbital time-scales in the ring are short (e.g. a few tens of Myr). In order to perform the age dating, it is therefore imperative that one uses tracers that are sensitive to these time-scales. The most widely used diagnostic for this purpose is the H α emission line. There are several reasons why this line is a popular choice. First, it is an optical emission line that can easily be measured. Second, its equivalent width (EW) decreases almost monotonically with time for an instantaneous burst allowing one to determine the evolutionary stage of a cluster from the EW value alone. The use of this emission line, however, is limited to clusters in the age range between 3 and 10 Myr, and therefore any inferred age differences have to be small (few Myr). Below 3 Myr, the EW of the H α is almost constant, and above 10 Myr the

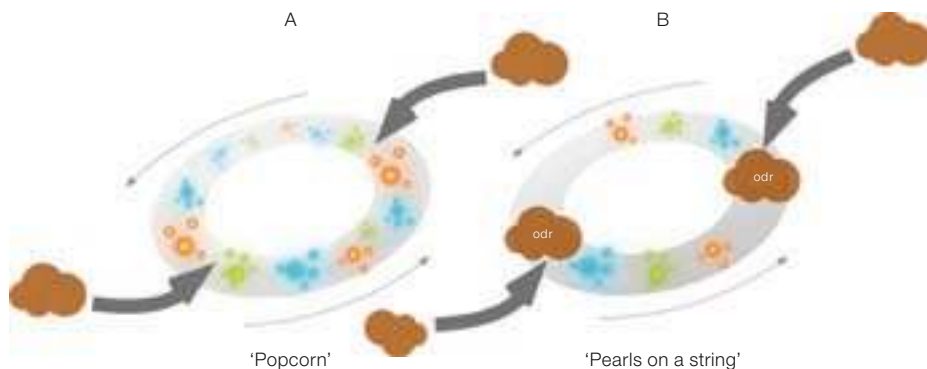


Figure 3: Two possible scenarios describing how star formation progresses along a nuclear ring. **Left:** the *popcorn* model, where star formation occurs randomly along the ring. **Right:** the *pearls on a string* scenario, where the ages of the stellar cluster define two sequences of increasing age along the ring. (Courtesy of J. Paillet, ESA)

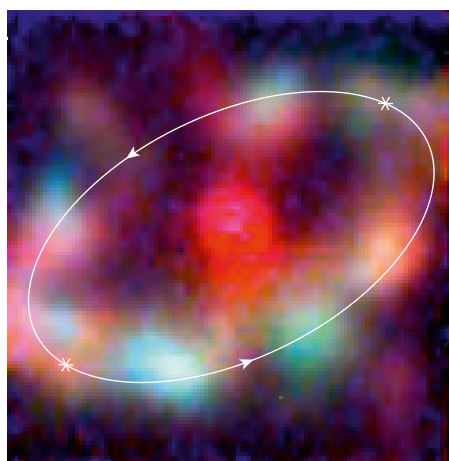


Figure 4: Evidence in support of the *pearls on a string* scenario in NGC 613. **Left:** *HST F666W* image. **Right:** HeI-Bry-FeII (blue-green-red) composite image of NGC 613 nuclear ring. Solid ellipse lines mark the location of the ring, star symbols the positions of the over-dense regions (ODRs), and arrows the sense of rotation of the stars and gas in the galaxy.

lates around it with no preferred location. Once a critical density is reached, the gas becomes unstable to gravitational collapse and star formation is triggered. In this model, individual hot spots collapse at random times and locations within the ring, and therefore there is no systematic age sequence. In the figure (left plot) the different starbursts are denoted by the star symbols and the different colours indicate different ages of the hot spots. In the second scenario (right), gas enters the ring at the intersection between the bar major axis and the inner Lindblad resonance. Downstream from this location, at the so-called over-density region (ODR), the gas density becomes sufficiently high to ignite star formation in a short-lived burst. A young cluster formed there will continue its orbit around the ring, but star formation will cease as soon as the first supernova explosions expel the gas. A series of starbursts triggered in the ODR will then produce a sequence of star clusters that

enter the ring like *pearls on a string*. In this scenario, the star clusters should show a bipolar age gradient along the ring, with the youngest clusters found close to the ODR, and increasingly older cluster ages in the direction of rotation, up to the opposite ODR. This is shown in the figure, where the colour sequence blue-green-red denotes clusters with increasing age.

In Figure 4 we put these two models to the test by showing the observations for NGC 613. In the left panel we display an *F666W HST* image of the nuclear regions. The ring is outlined with an ellipse, and two star symbols mark roughly the positions of the ODRs (based on the regions with highest dust extinction in the ring). In the right panel we present a false-colour image constructed from the SINFONI emission line maps of HeI, Bry, and [FeII] assigned to the blue, green, and red colour channels, respectively. The bottom half of the ring shows the trends ex-

pected under the *pearls on a string* picture: an age sequence (blue-green-red) in the different hot spots. The sequence is less obvious in the top part of the ring due to the strong interaction between the ring and the radio jet. In the full sample, not shown here, three out of five galaxies show some evidence for an age gradient of hot spots along the ring, while the remaining two galaxies have incomplete information and thus are consistent with either model.

A more detailed account of the results presented here can be found in Böker et al. (2007).

References

Böker T. et al. 2007, AJ, in press
 Buta R. and Combes F. 1996, Fund. Cosmic Physics 17, 95
 Hummel E. et al. 1987, A&A 172, 51
 Knapen J. et al. 2006, A&A 448, 489
 Rossa J. et al. 2006, AJ 132, 1074